

A quantitative DSC analysis of the metastable phase behavior of the sucrose–water system

J.E.K. Schawe*

Mettler-Toledo AG, Sonnenbergstrasse 74, CH-8603 Schwerzenbach, Switzerland

Received 10 June 2006; received in revised form 17 August 2006; accepted 26 September 2006

Available online 4 October 2006

Abstract

The phase behavior of the sucrose–water system is investigated using a quantitative calorimetric analysis. On the basis of a thermodynamic discussion of the melting behavior of the crystalline water component, the composition of the metastable amorphous phase and the so-called maximum freeze-concentrated composition were determined. This metastable phase can be described in a first approximation as an association complex consisting of one molecule of sucrose and five molecules of water which are held together by hydrogen bonding. The critical mass fraction of sucrose is thus 0.792. Furthermore, the origin of the different transitions in the aqueous phase is discussed. By analyzing the ice melting, an analytical relationship of the water activity coefficient is derived from the experimental data.

© 2006 Elsevier B.V. All rights reserved.

Keywords: Glass transition; Metastable structure; Water activity coefficient; Sucrose; Carbohydrate

1. Introduction

The equilibrium phase behavior of aqueous carbohydrate systems may be a simple eutectic system. Because of the kinetically hindered crystallization processes of the carbohydrates and their influence on the water crystallization, metastable phases occur even under relatively slow cooling conditions. Depending on the cooling and storage conditions, different unstable phases can form and transform to each other. These processes can be connected with phase separation. Consequently, the technically interesting metastable phase diagram of such systems becomes complex. The metastable phases are non-equilibrium microcrystals and amorphous glasses [1].

If the carbohydrate–water system is rapidly cooled from the equilibrated liquid to sufficient low temperatures, no crystallization occurs. The mixture is therefore in the glassy state. The glass transition temperature of the mixture depends from the concentration of the carbohydrate. With increasing carbohydrate concentration, the glass transition temperature increases [2]. The water acts as a plasticizer for the amorphous carbohydrate. This

glass transition temperature represents line T_g in the schematic phase diagram shown in Fig. 1.

The liquidus line of the water-rich mixture (also called melting point curve or freezing curve), T_{lw} , is expanded to a mass fraction larger than the eutectic concentration, due to the non-equilibrium origin of the related structures [1]. The liquidus line T_l (solute solubility curve) meets the melting point curve at the eutectic point T_e . Two additional transitions, T_1 and T_2 , are often reported in the literature. The lower transition T_1 is interpreted as the glass transition of the maximally freeze-concentrated glass [3]. The transition T_2 represents the onset of ice melting [4]. In the region between T_g and T_1 , phase separation and reorganization can occur depending on the thermal history of the sample. This is the region of unstable phases, which could be finally transformed to the metastable phase.

A focal point of interest in the phase diagram in Fig. 1 is related to the critical concentration $w_{s,c}$ [1], which is the mass fraction of the “maximally freeze-concentrated” amorphous water, and the related glass temperature in $T_{g,c}$.

This interpretation of the phase diagram in Fig. 1 is widely accepted in the literature, besides a controversial discussion about the origin of the transition T_2 [5–8].

In Fig. 1, the region around the critical point ($w_{s,c}$, $T_{g,c}$) is marked by an ellipsis. The phase behavior in this region is

* Tel.: +41 44 806 7438; fax: +41 44 806 7240.

E-mail address: Juergen.Schawe@mt.com.

Nomenclature

a	number of the “unfrozen” water molecules associated with a sucrose molecule
a_1	coefficient of the function Eq. (3) (extrapolated Δc_p for $x_s = 0$)
a_2	coefficient of the function Eq. (3) (extrapolated Δc_p for $x_s = 1$)
A	constant in Eq. (4)
B	slope in Eq. (4)
$c_{p,m}$	heat capacity contribution of water melting
Δc_p	intensity of the glass transition in J/(g K)
$\Delta c_{p,a}$	intensity of the glass transition of the pure association complex in J/(g K)
$\Delta c_{p,s}$	intensity of the glass transition of pure sucrose in J/(g K)
Δc_{p1}	intensity of the glass transition of the association complex in the mixture in J/(g K)
$\Delta c_{T_{m1}}$	height of the heat capacity step at begin of ice melting
$\Delta c_{p,a}^m$	intensity of the glass transition of the pure association complex in J/(mol K)
f	activity coefficient of water
g	osmotic coefficient of water
$\Delta h_{f,w}$	specific fusion enthalpy of pure water
Δh_w	specific fusion enthalpy of the water component
k	Gorgon–Taylor coefficient
m	sample mass
n_a	mole number of the association complex
n_s	mole number of sucrose
$n_{s,c}$	mole number of sucrose in the mixture at $x_{s,c}$
n_w	mole number of water
$n_{w,a}$	mole number of amorphous (“unfrozen”) water
$n_{w,s}$	mole number of water in the mixture at $x_{s,c}$
M_a	mole mass of the association complex
M_s	mole mass of sucrose
M_w	mole mass of water
R	gas constant
$T_{f,w}$	fusion temperature of pure water
T_g	glass transition temperature
$T_{g,c}$	glass transition temperature at $w_{s,c}$ (T_g of the maximum freeze solution)
$T_{g,s}$	glass transition temperature of pure sucrose
$T_{g,w}$	glass transition temperature of water
T_{g1}	glass transition temperature of the metastable amorphous phase
T_m	melting temperature of ice in the solution
T_{m1}	onset temperature of the ice melting in the mixture
T_{m2}	temperature of the liquidus line of water
ΔT_w	melting temperature depression of water
x_{aa}	molar fraction of the amorphous water in respect to the amorphous phase
x_s	molar fraction of sucrose

$x_{s,c}$	critical molar fraction of sucrose (sucrose mass fraction of the “maximum freeze solution”)
x_w	molar fraction of water
$x_{w,a}$	molar fraction of amorphous (“unfrozen”) water
x_0	coefficient of the function Eq. (3) (sucrose molar fraction on the inflection point)
Δx	coefficient of the function Eq. (3) (characterizes the step width)
$w_{w,a}$	mass fraction of water amorphous (“unfrozen”) water
w_s	mass fraction of sucrose
$w_{s,c}$	critical mass fraction of sucrose (sucrose mass fraction of the “maximum freeze solution”)
w_w	mass fraction of water

still under discussion. Frequently, $w_{s,c}$ is discussed as the mass fraction of sucrose at the intersection point of the glass transition curve T_g and the melting point curve Tlw [9–11]. In other references, the melting point curve finishes when it meets the temperature of the transition T2. The endpoint of the melting point curve is above the T_g curve. This occurs at the mass fraction $w_{s,c}$ at which the transition T1 meets the T_g curve [12,4]. Knowledge of the phase diagram in this region is highly important for understanding the thermodynamics and the structural changes of the non-equilibrium behavior of aqueous carbohydrate systems.

Another discussing point regarding the phase diagram is the origin of the glass with the glass transition temperature at T1. In the literature, we find different descriptions of the respec-

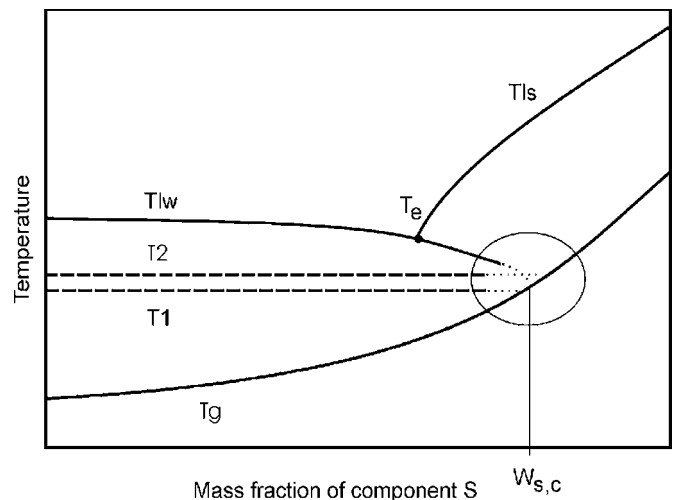


Fig. 1. Schematic phase diagram of a carbohydrate–water system. T_g is the curve of the glass transition of an amorphous system. Tlw is the liquidus line of the water-rich phase (melting point curve), Tls is the liquidus line of the carbohydrate-rich phase, T_e is the eutectic point, T1 is the low-temperature transition of the semicrystalline mixture with a minimum of amorphous water (glass transition of the maximally freeze-concentrated solution), T2 is the low-temperature transition of semicrystalline mixture (onset of ice melting), $w_{s,c}$ is the mass fraction of carbohydrate in the “maximally freeze-concentrated” solution.

tive structure, for example, “ice crystal dispersed within the continuous supersaturated solution phase” [14] or “amorphous solute/unfrozen water matrix surrounding the ice crystals in a frozen solution” [2].

On the basis of quantitative calorimetric measurements and evaluation in the framework of thermodynamics, we discuss and interpret the behavior of the phase diagram in the region around the critical point, the origin of the transition T1 and T2 and the composition of the maximally freeze-concentrated solution. The system we studied is sucrose–water.

The experimental data determined from the DSC curves of the slowly cooled mixtures are the characteristic temperatures of the thermal events T1, T2 and T1w. Furthermore, the related step heights of the heat capacity and melting enthalpy were determined. With an accurate determination of these data, all resulting evaluations and interpretations should be self-consistent. The interpretations presented in this paper are based on this condition.

2. Experimental

Aqueous solutions were prepared using HPLC grade de-ionized water. D(+)-Sucrose (99.5% GC) was obtained from Sigma–Aldrich Chemie GmbH. Up to a sucrose mass fraction of 0.65, crystallized sucrose was directly dissolved in the corresponding amount of water. Samples with a sucrose mass fraction between 0.65 and 0.8 were prepared by drying the 0.65 sucrose mass fraction solution in a vacuum oven for different times and at different temperatures. The concentration was determined from the mass loss. Samples with sucrose mass fractions above 0.95 were prepared directly in the DSC crucible. The appropriate amount of water was added, the crucible then hermetically sealed and the amount of water in the crucible measured. These samples were annealed at 60 °C for 1 day and afterwards heated at 5 K/min to above the melting temperature. The samples were then rapidly cooled by immediately removing them from the hot DSC furnace and placing them on a cold metal plate. All mass determinations were performed using METTLER TOLEDO balances. The MX5 was used for overall masses above 4 g. All larger masses were weighed using an AX26. Samples with a typical total mass of 15 mg were filled in the 40- μ L Al crucibles and hermetically sealed.

The calorimetric measurements were performed using a METTLER TOLEDO DSC823^e equipped with an HSS7 sensor and liquid nitrogen cooling. The HSS7 is a DSC sensor with high sensitivity and a relative short time constant especially in the low temperature region. The typical signal noise is of the order 0.2 μ W. This allows the accurate quantitative determination of the related values of the specific enthalpy of fusion or the change of the specific heat capacity at the glass transition even for weak thermal effects such as occur in dilute carbohydrate solutions.

Temperature calibration was performed using indium, water, octane and heptane. The enthalpy was calibrated using indium and water. The integral baseline was used to determine the enthalpy of ice melting.

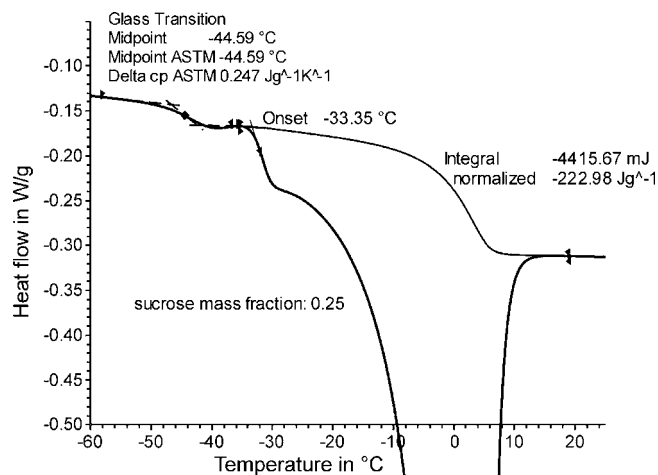


Fig. 2. Example of a DSC curve evaluation (exothermic upward). The glass transition of the metastable amorphous phase (transition T1), the onset of ice melting (transition T2) and the enthalpy of ice melting Δh_w were determined using the integral baseline.

Samples with a homogenous mixture were prepared by rapidly cooling the sample from a temperature above the respective melting temperature to -140 °C by placing it in the pre-cooled DSC cell. Samples with sucrose mass fractions above 0.65 were heated using a separate heater to above the melting temperature before cooling.

Samples with a metastable structure were obtained by cooling the sample from the equilibrated liquid to a temperature 30 K below the glass transition of the amorphous solution (T_g line in Fig. 1) or to -100 °C at 2 K/min.

All heating measurements were performed at 5 K/min.

From the glass transitions, the glass transition temperature, T_g , and the intensity of the glass transition, Δc_p , are determined. T_g is determined as the sample temperature at the inflection point of the heat flow step. Δc_p is the difference between the linear extrapolated heat capacity below and above the glass transition at T_g (see Fig. 2).

Because of the heat capacity difference between the solid and the liquid state of water, the commonly used linear base line results in systematic errors of the enthalpy determination by peak integration. Integral baselines [15] have therefore been used. Important for the enthalpy determination is the selection of the integration limits. A typical example is shown in Fig. 2. As the onset temperature for the peak integration a temperature is selected which is between the end of the glass transition and the onset of the transition T2. The prerequisite for this selection is the verifying of the prediction that T2 is caused by melting. This requires the self-consistency of all resulting data. By a preliminary data evaluation we found, that only integration limits as shown in Fig. 2, a melting enthalpy is evaluated, which is consistent to all other data, at using of a minimum number of assumptions about the structure of the amorphous component.

The characteristic temperature of transition T2 is determined as the onset temperature (Fig. 2). Furthermore, the step height at the melting onset $\Delta c_{p,melt}$ is determined.

The temperature of the liquidus line is determined from the peak maximum temperature. Because of heat transfer, the mea-

sured peak maximum temperature shifts to temperatures higher than the end temperature of the melting process. For a correct determination of the liquidus temperature, the melting curve of pure water was plotted versus the sample temperature. The region with an almost constant slope between the peak onset and the peak maximum was used to determine the slope of the curve. As described in reference [16], the maximum of the melting peak of the mixtures was corrected using a linear function with the same slope as that of the pure water peak.

3. Results and discussion

3.1. The homogenous amorphous mixture

3.1.1. The glass transition temperature

If a sucrose–water mixture is rapidly cooled from the liquid state to sufficiently low temperatures, the supercooled liquid mixture does not crystallize due to the limited maximum crystallization rate. It vitrifies at the glass transition at the “homogenous mixture”.

The measured glass transition temperatures as a function of the mass fraction of sucrose are shown in Fig. 3. The decrease of T_g with decreasing the sucrose concentration is typical if the solvent acts as a plasticizer. In such a case, the glass transition temperature as a function of the mass fraction can be describe by the Gordon–Taylor equation [17]:

$$T_g = \frac{w_s T_{gs} + k(1 - w_s) T_{gw}}{w_s + k(1 - w_s)} \quad (1)$$

where w_s is the mass fraction of sucrose. T_{gs} and T_{gw} are the glass transition temperatures of pure sucrose and water respectively in Kelvin. k is an empirical parameter. The glass transition of water was set to be $T_{gw} = 136$ K [18]. The other parameters were determined by curve fitting: $T_{gs} = 57$ °C and $k = 4.04$. These parameters are slightly different to the data published by Roos and Karel [19] ($T_{gs} = 62$ °C, $k = 4.7$) or Blond et al. [11] ($T_{gs} = 70$ °C, $k = 5.12$). The literature values of the glass transi-

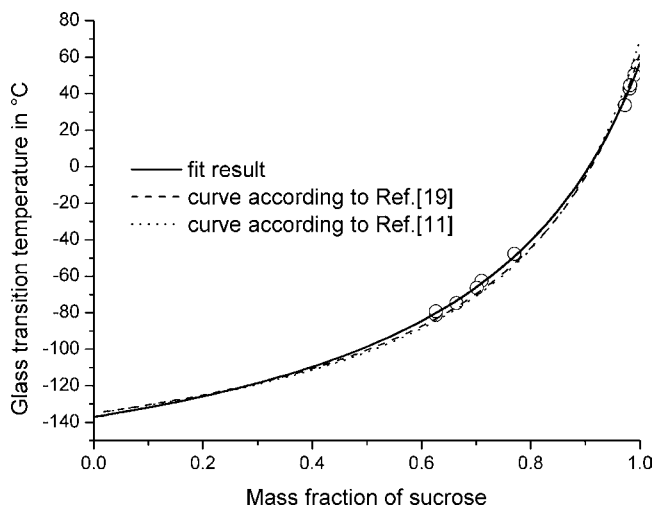


Fig. 3. Glass transition temperature of the homogeneous sucrose–water mixture as a function of the mass fraction of sucrose.

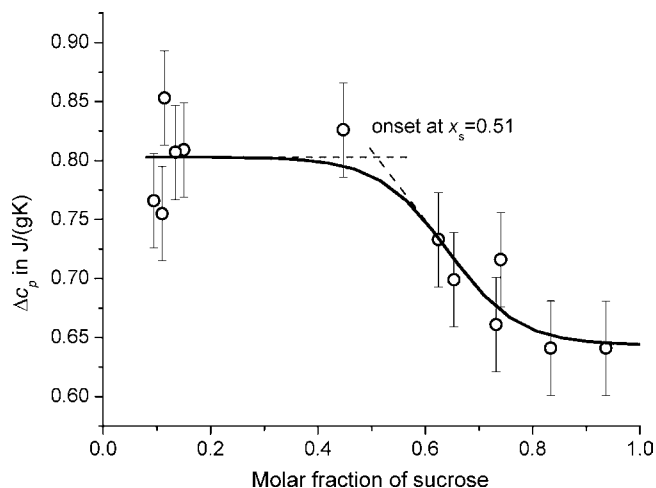


Fig. 4. Intensity of the glass transition as a function of the molar fraction of sucrose. The measured data are fitted with a sigmoidal function (Eq. (3)). The onset of the fit function is at $x_s = 0.51$.

tion temperature of pure sucrose differ between 52 and 70 °C [20].

To illustrate the differences in the glass transition temperatures, the related Gordon–Taylor curves are also plotted in Fig. 3. In the most interesting region around a sucrose mass fraction of 0.8, the difference between the literature data and our results are of the order 3–4 K. This difference in the measured data can be understood as being due to the influence of the different cooling rates on the measured glass transition temperature [21,22].

3.1.2. The intensity of the glass transition

The intensity of the glass transition Δc_p is the second important parameter that describes the glass transition. Roos and Karel [13] predicted a linear decrease of the glass transition intensity with increasing mass fraction of carbohydrate. We could not find such a dependence of the glass transition intensity on the composition of a sucrose–water mixture. To interpret our results, we plot the glass transition intensity as a function of the molar fraction of sucrose, x_s , instead of the commonly used mass fraction w_s (Fig. 4). The relation between both properties is given by

$$x_s = \frac{n_s}{n_s + n_w} = \frac{1}{1 + (M_s/M_w)((1/w_s) - 1)} \quad (2)$$

where n_s and n_w are the mole numbers of water and sucrose, and M_s , M_w are the related molar mass (342 and 18 g/mol, respectively).

It is shown in Fig. 4 that Δc_p for pure sucrose is of the order of 0.65 J/g K. With increasing water concentration in the mixture, the glass transition intensity increases and reaches an almost constant value. Such behavior can be describe by Eq. (3):

$$\Delta c_p = a_2 + \frac{a_1 - a_2}{1 + \exp((x_s - x_0)/\Delta x)} \quad (3)$$

The parameters of this function are determined to be $a_1 = 0.803$ J/g K, $a_2 = 0.644$ J/g K, $x_0 = 0.643$, $\Delta x = 0.065$ by curve fitting. The parameter, a_1 , is the intensity of the glass transition in the lower molar fraction range of sucrose. x_0 is the molar fraction at the inflection point of the fit curve and

Δx is a measure of the step width. The intensity of the glass transition of the pure sucrose is calculated from Eq. (3) to be $\Delta C_{ps} = 0.644 \text{ J/g K}$.

The curve in Fig. 4 suggests that the Δc_p is almost constant between a molar fraction of sucrose between 0.1 and 0.5. With higher molar fractions, Δc_p decreases to the value of pure sucrose. The onset in the $\Delta c_p(x_s)$ curve in Fig. 4 is determined to be 0.51. This is within the experimental limits identical to $x_s = 0.5$ and corresponds to a sucrose mass fraction of about $w_s = 0.95$. The glass transition intensity of sucrose increases if water is added and reaches a plateau at the ratio the sucrose and water molecules is 1:1. The reason for the change in Δc_p may be the hydrogen bonds between water and sucrose and the formation of associate complexes as a consequence of the hydrogen bonds. This result is also in agreement to the formation of a hydrogen bonded sucrose network. Such a percolation cluster structure should be formed above the threshold molar sucrose fraction, which is between 0.073 and 0.096 [23]. The change in the intensity of the glass transition is of the order 0.15 J/g K .

3.2. Determination of the phase diagram of the dilute sucrose solution

In this section we discuss the region of the phase diagram with a sucrose mass fraction of $w_s \leq 0.82$. Besides the glass transition of the supercooled homogenous mixture, different unstable phases occur in the sucrose–water system [24]. In the temperature region between the Gordon–Taylor line and the ice melting, glass transitions of amorphous sucrose–water mixtures can be measured. The related glass transition temperature depends on the actual amount of water in the glass. By phase separation, the amount of water in the amorphous phase can be increased during annealing, slow cooling or slow heating. As a consequence, the glass transition temperature of the resulting glass increases and the separated water crystallizes (“freezes”) [4]. At about -44°C , the glass transition temperature reaches a maximum. The related structure is metastable. It is usually referred to as “maximally freeze-concentrated” [2,12,19]. This means that the composition of the amorphous phase is almost stable and practically no further water crystallizes. Nevertheless, the stable equilibrium structure is the eutectic system [25].

The thermal behavior of different structures is shown in Fig. 5, using the mixture with a sucrose mass fraction of 0.664 as an example. The upper curve represents the homogenous mixture. The curve shows the glass transition of the homogenous mixture of water and sucrose at about -75°C (Gordon–Taylor temperature). At about -40°C a crystallization process occurs. Immediately after this the crystals melt. The total area of the crystallization and the melting peaks is zero. This indicates that in the initial sample, water and sucrose were mixed in an amorphous phase. After the rapid cooling, no water crystallized.

If the sample is cooled slowly (-2 K/min), partial phase separation occurs. Consequently, a certain amount of water has crystallized before the heating starts. Furthermore, a metastable amorphous phase was formed that undergoes a glass transition at

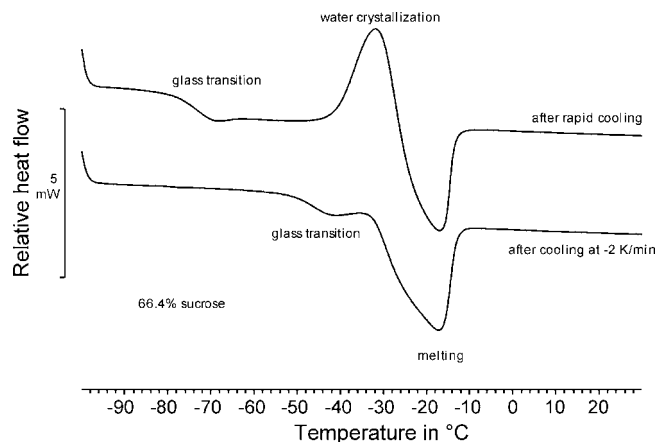


Fig. 5. DSC curves (exothermic upward) of the mixture with a sucrose mass fraction of 0.664 measured at 5 K/min .

about -44°C . Above this glass transition, the amorphous phase is liquid. In the presence of this liquid, the crystalline ice melts at about -20°C . The onset temperature of the melting peak is -34.5°C .

A selection of typical DSC curves for slowly cooled samples (cooling rate -2 K/min) with lower sucrose concentrations is shown in Fig. 6. Besides the melting peak, the curves show two endothermic steps which we refer to as transition T1 and transition T2. For clarification the relevant curve sections are shown in Fig. 6 diagram (A).

The transition T1 is identified as a glass transition. For all measured concentrations, this glass transition temperature, T_{g1} , is almost constant [4] -44°C . This is the glass transition temperature of the metastable glassy phase. This glass represents the amorphous component of the “maximally freeze-concentrated solution”.

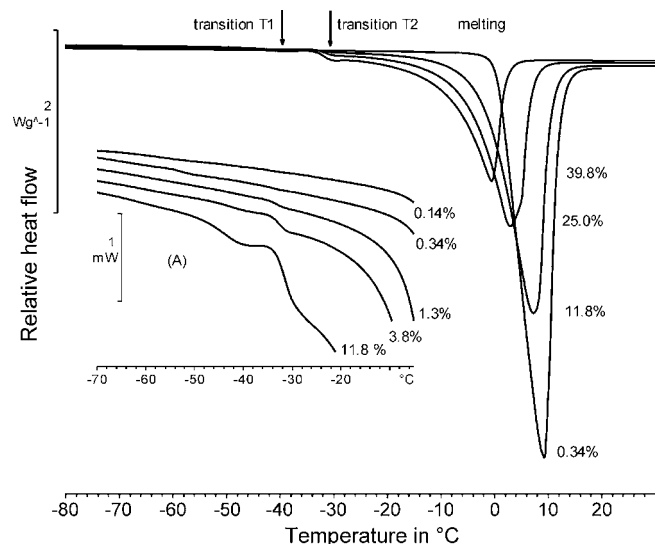


Fig. 6. DSC curves (exothermic upward) of different sucrose solutions measured at 5 K/min . The curves show two endothermic steps at about -44°C (transition T1) and -34°C (transition T2) and a melting peak. In diagram (A), the region in which transitions T1 and T2 occur are shown on an expanded scale for clarity.

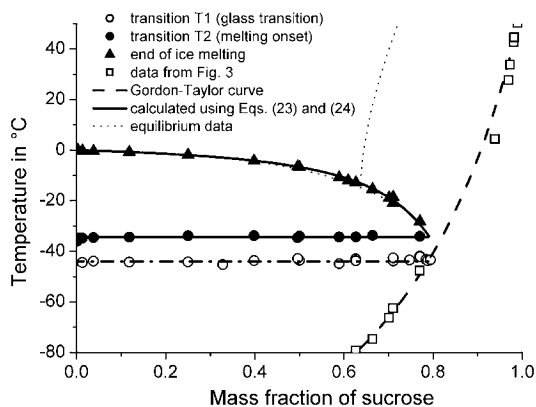


Fig. 7. Phase diagram of the aqueous part of the sucrose–water phase diagram. The equilibrium data for the liquidus lines (freezing point depression and solubility of sucrose in water) are taken from [25]. The Gordon–Taylor curve is taken from Fig. 3. The calculated liquidus line is determined using Eq. (23).

The transition T2 occurs around $-35\text{ }^{\circ}\text{C}$ for all samples. Following the common interpretation, this transition is the onset of the ice fusion in the liquid solution [4]. Recently, this transition has become the subject of controversial discussion mainly on the basis of temperature-modulated DSC measurements [5–8]. In these references, the transition is described as a glass process or as a combination of a glass transition and a fusion process. The intensity of this transition (step height) increases with increasing the sucrose content. Compared with a glass transition, the intensity is very large in case of high sucrose contents. For $w_s = 0.5$ the Δc_p intensity was determined to be 1.6 J/g K . This is too high for a glass transition. Because of this fact and the arguments presented in this paper we see no reason to discuss the existence of a glass process to describe this transition for our measurements. We therefore determine the characteristic temperature of transition T2 as the onset temperature of the step (Fig. 2). This is the onset of melting. The average characteristic temperature of this transition is determined to be $-34.4\text{ }^{\circ}\text{C}$.

The liquidus line of water is determined from the melting peak temperatures.

The phase diagram including the glass transition of the homogenous sucrose mixture (Gordon–Taylor behavior), the liquidus line determined from the main melting peak temperature and transitions T1 and T2 are shown in Fig. 7. For comparison, the equilibrium data for the liquidus lines (freezing point depression and solubility of sucrose in water) taken from [25] are also plotted.

3.3. Determination of the origin of the maximally freeze-concentrated solution

3.3.1. Methods to determine $w_{s,c}$

The critical concentration $w_{s,c}$ is also the mass fraction of sucrose in the metastable amorphous phases. In the literature, the critical concentration $w_{s,c}$ of the “maximally freeze-concentrated solution” is often determined from the intersection point of the glass transition temperature T_{g1} with

the Gordon–Taylor curve [4] or the liquidus line of water with the Gordon–Taylor curve [10,11,26]. The determination of the critical concentration using the fictive intersection between the glass transition line of the homogenous supercooled liquid and the liquidus line requires a very slow cooling experiment, because of the highly kinetically hindering of the phase separation close $w_{s,c}$. In addition to the problems due to the extrapolation of the liquidus line, the critical concentration determined by this method is not identical to the metastable associated structure measured by the experimental conditions used in the present paper.

Another method to determine $w_{s,c}$ on the basis of the Gordon–Taylor line is the determination of the intersection point of this line with the glass transition temperature at T1 of the metastable glass T_{g1} . Based on our measurements, we obtained a value of 0.789. This corresponds to the literature data between 0.641 and 0.830 [11].

The basic problem of the determination of w_s using the Gordon–Taylor line of the homogenous mixture is the cooling rate dependence of the glass transition temperature [21,22]. Glass transition temperature shifts of approximately $\pm 5\text{ K}$ are possible because of the different cooling rates used for the determination of the Gordon–Taylor curve and the glass transition of the metastable glass, T_{g1} . This yields values of $0.77 \leq w_{s,c} \leq 0.81$. This is the uncertainty for the critical concentration determined by the intersection method.

An alternative method to determine the critical composition, $w_{s,c}$, is based on the determination of the enthalpy of fusion of the crystallized water, Δh_w , by integration of the ice melting peak. This enthalpy decreases with increasing sucrose concentration. Several authors suppose a linear relation between Δh_w and the mass fraction of carbohydrate [27–29]. Using this method, the critical mass fraction of sucrose is determined by linear extrapolation to $\Delta h_w = 0$. For this method, the accuracy of the enthalpy determination is important. This can be increased by proper calibration, by optimizing the integration limits and by selection of the best baseline for the peak integration. In this case the integration has to begin before the transition T2 (Fig. 2).

The measured enthalpies of ice melting as a function of the mass fraction of sucrose are shown in Fig. 8. The fit of our data with the linear function:

$$\Delta h_w = A - Bw_s \quad (4)$$

yields $A = 333.6\text{ J/g}$ and $B = 428.1\text{ J/g}$ and finally a value of 0.779 for $w_{s,c}$. In molar units, this corresponds to $x_{s,c} = 0.156$. This value is higher than that reported by Furuki [29] ($w_{s,c} = 0.691$, $x_{s,c} = 0.105$). Comparison of the melting enthalpy data from Ref. [29] with the data in Fig. 8 shows that data from Ref. [29] for Δh_w is significantly lower than ours, especially at larger w_s (12% at $w_s = 0.4$). The reason for this may be the selection of a non-optimum baseline for peak integration or the relative high cooling rate of 8 K/min in Ref. [29]. This could initiate an incomplete phase separation. Consequently the water concentration in the amorphous phase is increased.

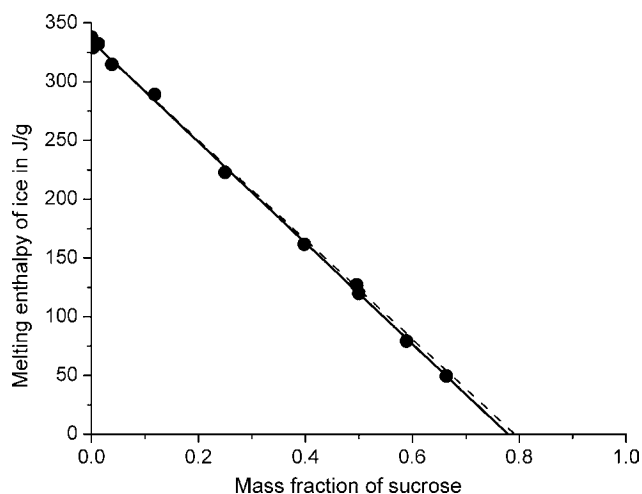


Fig. 8. Melting enthalpy of the crystalline water component as a function of the mass fraction of sucrose. The solid line represents the result of the curve fitting ($A = 333.6 \text{ J/g}$, $B = 428.1 \text{ J/g}$); the dashed line is given by the expected composition (see text) of the metastable structure ($A = 333.6 \text{ J/g}$, $B = 421.4 \text{ J/g}$).

3.3.2. The composition of the metastable amorphous sucrose–water phase

The relative amount of amorphous water is related to the melting enthalpy of ice:

$$\frac{w_{wa}}{w_w} = \frac{n_{wa}}{n_w} = \frac{x_{wa}}{x_w} = 1 - \frac{\Delta h_w}{w_w \Delta h_{f,w}} \quad (5)$$

where w_w and x_w are the mass fraction and the molar fraction of water in the mixture. w_{wa} , n_{wa} and x_{wa} are the related properties for the amorphous (“unfrozen”) water. $\Delta h_{f,w}$ is the specific enthalpy of fusion for pure water (333.57 J/g).

We assume that each sucrose molecule is associated with a water molecules in the amorphous phase:

$$n_{wa} = a n_s \quad (6)$$

From Eq. (6) follows:

$$\frac{n_{wa}}{n_w} = a \frac{n_s}{n_w} = a \frac{x_s}{x_w} \quad (7)$$

A combination of Eqs. (5) and (7) taken into account that $w_s = 1 - w_w$ and $x_s = 1 - x_w$ yields:

$$\Delta h_w = \Delta h_{f,w} \left(1 - a \frac{x_s}{1 - x_s} \right) (1 - w_s) \quad (8)$$

From Eq. (2) follows:

$$\frac{x_s}{1 - x_s} = \frac{M_w w_s}{M_s (1 - w_s)} \quad (9)$$

The final equation results from inserting of Eq. (9) into Eq. (8):

$$\Delta h_w = \Delta h_{f,w} - \left(\Delta h_{f,w} \left(1 + a \frac{M_w}{M_s} \right) \right) w_s \quad (10)$$

The critical molar fraction of sucrose at which all water is associated with sucrose is

$$x_{s,c} = \frac{n_{s,c}}{n_{s,c} + n_{w,c}} = \frac{n_{s,c}}{n_{s,c} + a n_{s,c}} = \frac{1}{a + 1} \quad (11)$$

It is obvious that Eq. (10) is an expression for the empirical linear Eq. (4). From the slope $B = 428.1 \text{ J/g}$, the average number of associated water molecules, $a = 5.37$, can be determined from Eq. (10). Taking into account the experimental errors, this is consistent with $a = 5$ (see dashed line in Fig. 8). Consequently, as a first approximation each sucrose molecule is associated with five water molecules, in the metastable phase. The critical concentration (or the concentration of the maximally freeze-concentrated fraction) is $x_{s,c} = 1/6$ or $w_{s,c} = 0.792$. This value is in a good agreement with the commonly discussed results (see above).

Several authors propose that the unfrozen region of the solution consists of water molecules which form hydrogen bonds with the OH groups of sucrose [30–32]. However, the expected number of the related hydroxyl groups of the sucrose molecule differs as follows:

- (i) Model calculations of the molecular dynamics in dilute solutions result in one sucrose molecule, encapsulated by a shell of water molecules engaged in hydrogen bonding of each of the eight hydroxyl groups [31] (8 mol of water and 1 mol of sucrose) and also
- (ii) proposes six free OH groups and one indirect intramolecular hydrogen bond due to a hydrogen bonding of one water molecule with two sucrose OH groups [31] (7 mol of water and 1 mol of sucrose).
- (iii) Furthermore, the formation of one intramolecular hydrogen bond is proposed [32] (6 mol of water and 1 mol of sucrose). This structure is close to the equatorial OH model [30] which predicts 6.3 mol of water and 1 mol of sucrose.
- (iv) Our result is consistent with the formation of a shell of five water molecules surrounding a sucrose molecule. This finding is in agreement with two intramolecular hydrogen bonds as in the crystalline structure [33].

For description of the experimental data we use an association model for the structure of the metastable sucrose–water system. We start with a solution, which is rapidly cooled below the glass transition of the homogenous mixture. Because of the kinetically hindering in the glassy state practically no phase separation and ice crystallization occur in the time scale of the experiment. By heating above the glass transition temperature, water crystallizes if it is not bonded by hydrogen bonds with sucrose. This phase separation reduces the water concentration in the amorphous phase and increases therefore the glass transition temperature. A sucrose molecule bonds maximally eight water molecules. However, the hydrogen bonds are not infinite long stable. Because of fluctuations water molecules becomes free and crystallize, if the mobility is large enough before it forms again hydrogen bonds with sucrose. Consequently, the sucrose concentration increases with this annealing process in the liquid phase. This increases the probability of intramolecular hydrogen bonds in the sucrose molecule. Obviously, the characteristic live time of the associates increases with reducing the water concentration in the amorphous phase. This means that the probability of water molecules to form again hydrogen bonds with sucrose, before crystallization occurs, becomes high

in comparison to the possibility that the water becomes a part of an ice crystal. In this case the average characteristic time of an association is larger than the time of investigation. The association becomes metastable. For the presented measurements this metastable association has in average five water molecules and one sucrose molecule. This model is consistent with the results of Mathlouthi [34], which indicate a concentration dependence of the sucrose conformation with no intramolecular hydrogen bonds in dilute solutions and the tendency for formation of such hydrogen bonds at higher concentrations.

The characteristic life time of the metastable association depends on the sucrose concentration, the temperature and the actual structure of the ice-amorphous compound. At lower sucrose concentration and increasing temperature the lifetime decreases. The further reduction of the water concentration yields to an increase of the glass transition temperature at T_1 and a decrease of the onset temperature of melting at sufficient long experimental time. In this point this model is consistent to the discussion of Goff et al. [7].

3.3.3. Analysis of the glass transition intensity of the amorphous association complex

It is assumed above that all the sucrose molecules are present in the amorphous phase. This assumption is supported by the intensity of the glass transition of the metastable association complex. The measured glass transition intensity (step height of the specific heat capacity at the glass transition at $-44\text{ }^\circ\text{C}$), Δc_{p1} , is related to the glass transition intensity of the pure association complex (5 mol water and 1 mol sucrose), $\Delta c_{p,a}$ and the concentration of the association complex in the sample:

$$\Delta c_{p1} = \frac{\Delta c_{p,a}^m n_a}{m} = \frac{\Delta c_{p,a}^m n_a}{n_s M_s} w_s \quad (12)$$

where $\Delta c_{p,a}^m$ is the molar specific heat capacity of the pure association complex, n_a the molar number of the association complex in the sample and m is the sample mass. The relation between the molar specific heat capacity and the specific heat capacity of the association complex is

$$\Delta c_{p,a}^m = \Delta c_{p,a} M_a \quad (13)$$

The molar mass of the association, M_a , is with respect to Eq. (6):

$$M_a = M_s + a M_w \quad (14)$$

where M_w is the molar mass of water. Inserting Eqs. (13) and (14) into Eq. (12) yields:

$$\Delta c_{p1} = \Delta c_{p,a} \left(1 + a \frac{M_w}{M_s} \right) \frac{n_a}{n_s} w_s \quad (15)$$

The measured glass transition intensities versus the mass fraction of sucrose are plotted in Fig. 9. The best fit delivers a slope of 1.005 J/g K . $\Delta c_{p,a}$ is assumed to have a value of 0.803 J/g K as derived from the fit curve in Fig. 4 at the critical molar fraction ($x_{s,c} = 1/6$). After inserting the molar masses and $a = 5$ into Eq. (15), it follows that the ratio of the molar numbers $n_a/n_s = 0.991$.

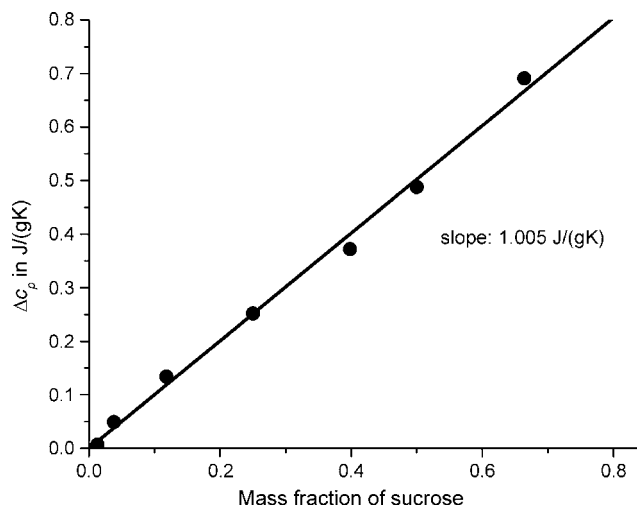


Fig. 9. Intensity of the glass transition of the amorphous association complex as a function of the mass fraction of sucrose. The fit with a linear function through the origin yields a slope of 1.005 J/g K .

For the metastable association complex we can therefore set:

$$n_a = n_s \quad (16)$$

This result is an indication that each sucrose molecule is incorporated in the amorphous metastable association complex which contains $1/6$ molar fraction of sucrose and $5/6$ molar fraction of water.

3.4. Ice melting and water activity

The dependence of the melting temperature of ice, T_m , on the sucrose content can be described at [35]:

$$\frac{\Delta h_{f,w} M_w}{R} \left(\frac{1}{T_{f,w}} - \frac{1}{T_m} \right) = \ln(x_w f) = g \ln x_w \quad (17)$$

where f is the activity coefficient and g is the osmotic coefficient of water. Both coefficients describe the interaction between the water and the sucrose molecules. In this equation, the influence of the heat capacity change in the liquid and the solid phase is neglected. The relation between the coefficients follows from Eq. (17):

$$g = 1 + \frac{\ln f}{\ln x_w} \quad (18)$$

After substitution of $T_m = T_{f,w} - \Delta T_w$ and $x_w = 1 - x_s$ in Eq. (17) and using $T_{f,w}^2 \approx T_{f,w}(T_{f,w} - \Delta T_w)$ and $\ln(1 - x_s) \approx -x_s$ (for small molar fractions) Eq. (17) is simplified to

$$\Delta T_w = - \frac{RT_{f,w}^2}{\Delta h_{f,w} M_w} g x_s \quad (19)$$

The osmotic coefficient, g , can be calculated from the measured melting temperature depression using Eq. (19). Fig. 10 shows the experimental data of g as a function of the molar fraction of sucrose.

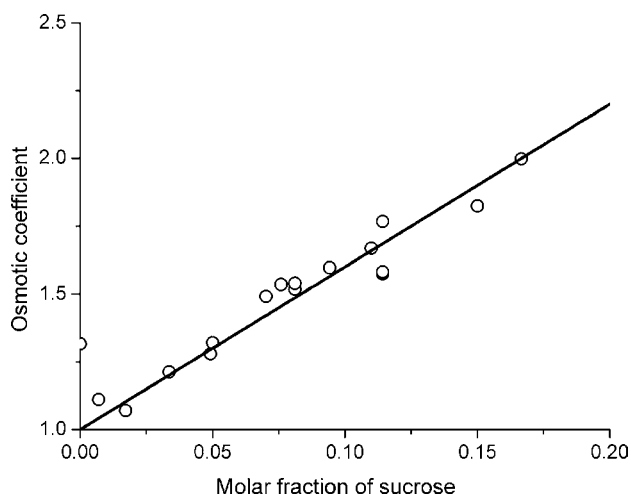


Fig. 10. Osmotic coefficient, g , as a function of the molar fraction of sucrose, x_s . The line represents Eq. (20).

As shown in Fig. 10, the experimental data follows the linear function:

$$g = (a + 1)x_s + 1 \quad (20)$$

with $a = 5$. According to Eqs. (6) and (11), the osmotic coefficient can be expressed by

$$g = 1 + \frac{x_{wa}}{x_w} = 1 + \frac{x_s}{x_{s,c}} \quad (21)$$

Eq. (21) shows that $g - 1$ can be interpreted as the proportionality factor between the molar fraction of the amorphous water bound in the association complex and the total molar fraction of water.

According to Eq. (18) the activity coefficient of water, f , is obtain by inserting Eq. (21):

$$f = (1 - x_s)^{x_s/x_{s,c}} \quad (22)$$

In the context of this paper Eq. (22) has no adjustable parameter because the critical molar fraction is $x_{s,c} = 1/6$. To prove the consistency of this equation with the experimental data, the measured water activity coefficient as a function of the molar fraction of sucrose was fitted using Eq. (22) with the critical molar fraction, $x_{s,c}$, as the only fit parameter (Fig. 11). The curve of the best fit is also shown in Fig. 11. The fit parameter is $x_{s,c} = 0.170$. This is in excellent agreement with the predicted value of 0.167. Consequently, we recommend Eq. (22) as a phenomenological equation for the water activity coefficient in a sucrose solution.

Using Eqs. (22) or (21) and the knowledge of the critical concentration, we can describe the aqueous part of the phase diagram in Fig. 7. Eq. (21) can be inserted in Eq. (22) to calculate the liquidus line. The equation of the liquidus line of water, T_{m2} , is then

$$T_{m2} = T_{f,w} - \Delta T_w = T_{f,w} - \frac{RT_{f,w}^2}{\Delta h_{f,w}M_w} \left(1 + \frac{x_s}{x_{s,c}}\right) x_s \quad (23)$$

The beginning of the ice melting, T_{m1} , is identical with transition T2 discussed in Section 1. The temperature of this transition can

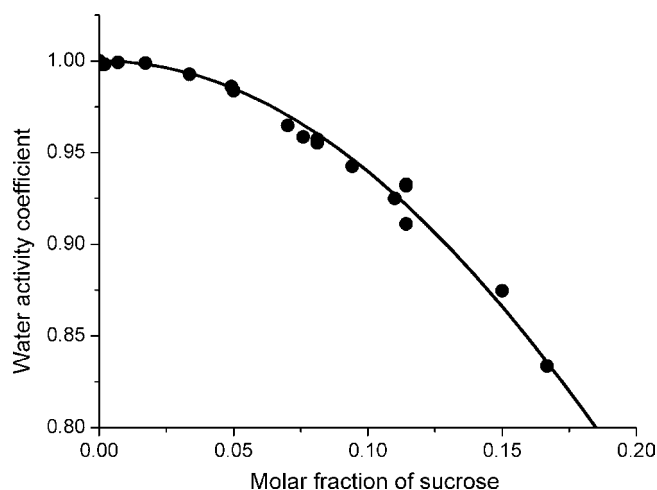


Fig. 11. The water activity coefficient as a function of the molar sucrose fraction. The solid line represents the best fit curve using Eq. (22). The fit parameter is $x_{s,c} = 0.170$.

be calculated using Eq. (23) by inserting $x_{s,c}$ for the sucrose mass fraction:

$$T_{m1} = T_{f,w} - \frac{RT_{f,w}^2}{\Delta h_{f,w}M_w} 2x_{s,c} \quad (24)$$

with $x_{s,c} = 1/6$ it follows from Eq. (24) that $T_{m1} = -34.3^\circ\text{C}$. The averaged measured temperature of T_{m1} is -34.4°C . The curves of T_{m1} and T_{m2} are plotted in the phase diagram in Fig. 7. This figure shows the excellent agreement between the theoretical curves and the measured data.

3.5. The step-height of the begin of melting at T_2

Another parameter, which we analyzed, is the step height at the onset of melting, $\Delta c_{T_{m1}}$. If the thermal event T2 is the onset of ice melting at presents of the liquid sucrose–water association, $\Delta c_{T_{m1}}$ can be calculated from the liquidus line according to Eq. (23).

The contribution of the apparent heat capacity, $c_{p,m}$, due to water melting is

$$c_{p,m} = \Delta h_{f,m} \left(\frac{dx_{wa}}{dT} \right)_p \quad (25)$$

For the calculation of this heat capacity contribution we define the molar fraction of water in the amorphous phase, x_{aa} :

$$x_{aa} = \frac{n_{wa}}{n_{wa} + n_s} \quad (26)$$

where n_{wa} is the molar number of water in the metastable amorphous phase. At the beginning of the melting, at $T \leq T_{m1}$, this molar fraction is $x_{aa} = 1 - x_{s,c}$. After complete melting is $x_{aa} = x_w$. During the melting process, x_{aa} increases with increasing temperature. Substitution of x_s with $1 - x_{aa}$ in Eq. (23) and rearrangements yield to

$$x_{aa}(T) = 1 + \frac{x_{s,c}}{2} - \sqrt{\left(\frac{x_{s,c}}{2}\right)^2 + \frac{\Delta h_{f,w}M_w}{RT_{f,w}} x_{s,c}(T_{f,w} - T)} \quad (27)$$

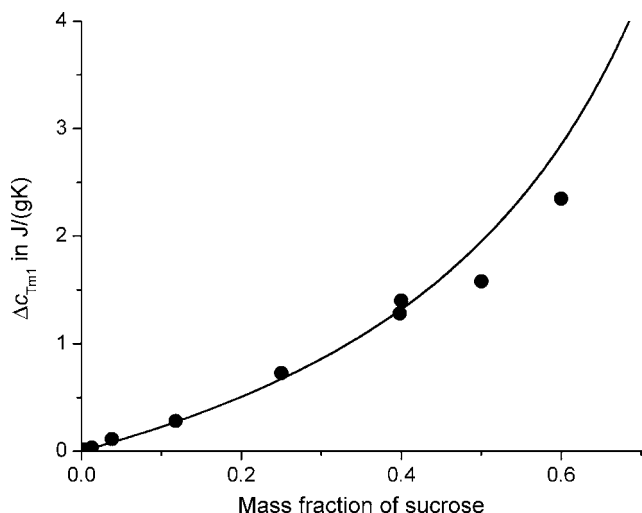


Fig. 12. Step height of the apparent heat capacity at begin of ice melting as a function of the sucrose mass fraction. The solid line represents the expected curve according to Eq. (29); the symbols are the measured data.

The relation between x_{wa} and x_{aa} is given by

$$x_{wa} = \frac{x_{aa}(1 - x_w)}{1 - x_{aa}} \quad (28)$$

Inserting of Eqs. (28) and (27) in Eq. (25) and consideration of Eq. (24) delivers the expected step-height at the melting onset:

$$\Delta c_{T_{m1}} = c_{p,m}(T_{m1}) = \Delta h_{f,m} \left. \frac{dx_{wa}}{dT} \right|_{T_{m1}} = \frac{\Delta h_{f,m}^2 M_w}{3T_{f,w} x_{s,c}^2} (1 - x_w) \quad (29)$$

The step-height of the heat capacity at the melting onset should follow a linear function versus the water molar fraction. In Fig. 12 the expected values (according to Eq. (29)) are compared with the measured data versus the mass fraction of sucrose. Up to $w_s \leq 0.4$ the measured data agree well with the predictions. At larger sucrose concentrations the measured values are lower than expected. The reason of this deviation is that the kinetics of the phase separation during cooling is slowing down at higher sucrose concentration. Thus, the real sucrose concentration in the amorphous phase after cooling with 2 K/min is lower than the critical concentration. In this concentration range a lower cooling rate is necessary to reach $x_{s,c}$ in the amorphous phase. This result is a further independent indication, for the interpretation of the transition T2 as melting onset and for the existence of the discussed critical association.

4. Conclusion

At fast cooling rates, a glass transition of the homogenous mixed solution occurs. The related glass transition temperature strongly depends on the composition and follows the Gordon–Taylor equation.

If the material is slowly cooled, a transition T1 occurs at -44.0°C . This is the glass transition of a metastable association complex. The structure of this complex is normally characterized by the critical mass fraction, $w_{s,c}$. The methods commonly

used to determine $w_{s,c}$ are (i) the Gordon–Taylor equation or (ii) the extrapolation of the melting enthalpy of ice as a function of the mass fraction to $\Delta h_w = 0 \text{ J/g}$. Method (i) is connected with uncertainty due to the cooling rate dependence of the glass transition. At first sight method (ii) seems to be phenomenologically correct. However, it is not related to the structure of the molecular association. Based on the assumption that in the average a water molecules are associated with each sucrose molecule, a linear equation between the specific melting enthalpy of the remaining ice and the mass fraction of sucrose was derived. The result is that the metastable association complex has in the average a composition of one molecule sucrose and five molecules water. This is also the composition of the “maximum freeze concentrated” compound of the amorphous phase and the ice. The critical concentration is therefore related to $x_{s,c} = 0.167$ or $w_{s,c} = 0.792$. The metastable association complex is a result of phase separation during cooling and storage above the glass transition of the actual amorphous phase.

The transition T2 at -34.4°C is the onset of ice melting at the presence of the amorphous association complex of sucrose and water. Evidence for an overlap with a glass process could not be found. In contrast, the analysis of the melt behavior in the framework of thermodynamics of associated solutions show that this transition is only related to a melting process for the analyzed conditions.

Using the thermal event, which is related to the liquidus line (melting point curve) of water, the osmotic and activity coefficients of water are determined. The activity coefficient strongly depends on the relative amount of amorphous water. An empirical expression was obtained for the concentration dependence of the activity coefficient. At the critical concentration, the activity coefficient is identical to the mole fraction of water. Using this relationship of the activity coefficient, the melting behavior of water in the sucrose melt can be described in the region of $0 \leq w_s \leq w_{s,c}$.

Based on the experimental results, we conclude that the formation of the metastable amorphous phase is a result of conformational fluctuations of the sucrose molecules.

The use of quantitative DSC analysis and an at least self-consistent evaluation and interpretation of all measurable effects can improve understanding of metastable phase behavior of aqueous carbohydrate systems.

Acknowledgments

The author thanks his colleagues Rudolf Riesen and Markus Schubnell (METTLER TOLEDO) for helpful discussions.

References

- [1] A.P. MacKenzie, Phil. Trans. R: Soc. Lond. B 278 (1977) 167–189.
- [2] L. Slade, H. Levine, J. Food Eng. 24 (1995) 431–509.
- [3] H. Levine, L. Slade, J. Chem. Soc., Faraday Trans. 1 4 (1988) 2619.
- [4] Y. Roos, M. Karel, Int. J. Food Sci. Technol. 26 (1991) 553.
- [5] S.A. Knopp, S. Chongprasert, S.L. Nail, J. Therm. Anal. 54 (1998) 659–672.
- [6] S.R. Aubuchon, L.C. Thomas, W. Theuerl, H. Renner, J. Therm. Anal. 52 (1998) 53–64.

- [7] H.D. Goff, E. Verespej, D. Jermann, *Thermochim. Acta* 399 (2003) 43–55.
- [8] H.D. Goff, *Pure Appl. Chem.* 67 (1995) 1801–1808.
- [9] F. Franks, N. Murase, *Pure Appl. Chem.* 64 (1992) 1667–1672.
- [10] J. Liesbach, T. Rades, M. Lim, *Thermochim. Acta* 401 (2003) 159–168.
- [11] G. Blond, D. Simatos, M. Catte, C.G. Dussap, J.B. Gros, *Carbohydr. Res.* 298 (1997) 139–145.
- [12] Y. Bai, S. Rahman, C.O. Perera, B. Smith, L.D. Melton, *Food Res. Int.* 34 (2001) 89–95.
- [13] Y. Roos, M. Karel, *Cryo-Letters* 12 (1991) 367–376.
- [14] F. Franks, *Pure Appl. Chem.* 65 (1993) 2527–2537.
- [15] B. Wunderlich, *Thermal Analysis*, Academic Press, Boston, 1990, pp. 277–280.
- [16] G.W.H. Höhne, in: V.B.F. Mathot (Ed.), *Calorimetry and Thermal Analysis of Polymers*, Hanser Publishers, Munich, 1994, pp. 80–82.
- [17] M. Gordon, J.S. Taylor, *J. Appl. Chem.* 2 (1952) 493–500.
- [18] G.P. Johari, A. Hallbrucker, E. Meyer, *Nature* 330 (1987) 552–553.
- [19] Y. Roos, M. Karel, *Int. J. Food Sci. Technol.* 26 (1991) 553–566.
- [20] R. Urbani, F. Sussich, S. Prejac, A. Cesàro, *Thermochim. Acta* 304/305 (1997) 359–367.
- [21] J.E.K. Schawe, *J. Polym. Sci., Part B: Polym. Phys.* 36 (1998) 2165.
- [22] R. Wungtanagorn, S.J. Schmidt, *Thermochim. Acta* 369 (2001) 95–116.
- [23] V. Molinero, T. Cagin, W.A. Goddard, *Chem. Phys. Lett.* 377 (2003) 469–474.
- [24] L. Slade, H. Levine, *Pure Appl. Chem.* 60 (1988) 1841–1864.
- [25] Z. Bubnik and P. Kadlec, in: M. Mathlouthi, P. Reiser (Eds.), *Sucrose: Properties and Application*, Blackie Academic & Professional, London, 1995, pp. 101–125.
- [26] R.H. Hartley, C. van den Berg, F. Franks, *Cryo-Letters* 12 (1991) 113–124.
- [27] Y. Roos, M. Karel, *J. Food Sci.* 56 (1991) 266–267.
- [28] P.J.A. Sobral, V.R.N. Telis, A.M.Q.B. Habitate, *Thermochim. Acta* 376 (2001) 83–89.
- [29] T. Furuki, *Carbohydr. Res.* 337 (2002) 441–450.
- [30] H. Kawai, M. Sakurai, Y. Inoue, R. Chujo, S. Kobayashi, *Cryobiology* 29 (1992) 599–606.
- [31] S. Immel, F.W. Lichtenthaler, *Liebigs Ann.* (1995) 1925–1937.
- [32] E.S. Stevens, C.A. Duda, *J. Am. Chem. Soc.* 113 (1991) 8622–8627.
- [33] J.C. Hanson, L.C. Sieker, L.H. Jensen, *Acta Crystallogr. Sect. B* 29 (1973) 797–808.
- [34] M. Mathlouthi, *Carbohydr. Res.* 91 (1981) 113–123.
- [35] R. Haase, *Thermodynamik der Mischphasen*, Springer-Verlag, Berlin, 1956.